Uranium Uptake in Paracentrotus lividus Sea Urchin, Accumulation and Speciation

Benjamin Reeves, Maria Rosa Beccia, Pier Lorenzo Solari, Danil Smiles, David Shuh, C. Berthomieu, Didier Marcellin, Nicolas Bremond, Luisa Mangialajo, Sophie Pagnotta, et al.

Uranium uptake in Paracentrotus lividus sea urchin, accumulation and speciation

Journal:	*Environmental Science & Technology*
Manuscript ID	es-2018-06380c.R1
Manuscript Type:	Article
Date Submitted by the Author:	10-May-2019
Complete List of Authors:	Reeves, Benjamin; Universite Cote d'Azur, ICN Beccia, Maria Rosa; Universite Cote d'Azur, Institut de Chimie de Nice Solari, Pier Lorenzo; Synchrotron Soleil, Smiles, Danil; Chemical Sciences Division, Glenn T. Seaborg Center Shuh, David; Chemical Sciences Division, Glenn T. Seaborg Center Berthomieu, Catherine; CEA-Cadarache, Laboratoire des Interactions Protéine Métal Marcellin, Didier; CEA-Cadarache, Laboratoire des Interactions Protéine Métal Bremond, Nicolas; CEA, DRF/BIAM Passeron Mangialajo, Luisa; COMUE Sorbonne Universites; Universite Cote d'Azur, Ecomers Pagnotta, Sophie; Universite Cote d'Azur, CCMA Monfort, Marguerite; CEA DAM Ile de France Moulin, Christophe; CEA DAM Ile de France Den Auwer, Christophe; Universite Cote d'Azur, ICN

Uranium uptake in *Paracentrotus lividus* sea urchin, accumulation and speciation

Benjamin Reeves[1,7], Maria Rosa Beccia[1], Pier Lorenzo Solari[2], Danil E. Smiles[3], David K. Shuh[3], Catherine Berthomieu[4], Didier Marcellin[4], Nicolas Bremond[4], Luisa Mangialajo[5,6], Sophie Pagnotta[8], Marguerite Monfort[7], Christophe Moulin[7], Christophe Den Auwer[1]

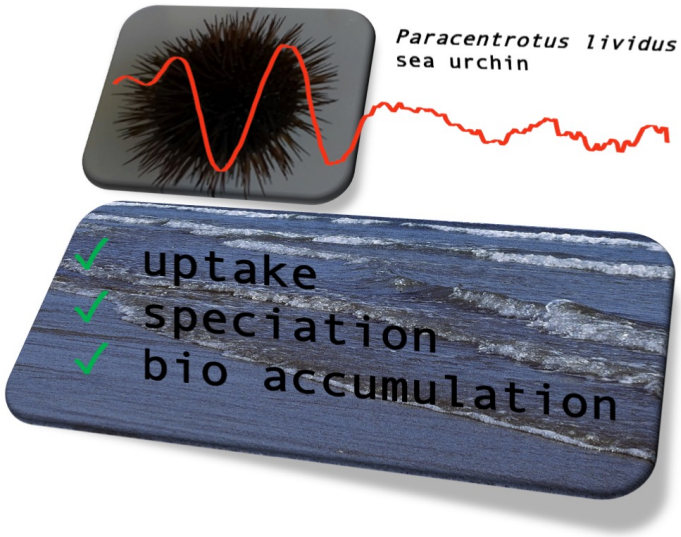

Uranium uptake in *Paracentrotus lividus* sea urchin, accumulation and speciation

Benjamin Reeves[1,7], Maria Rosa Beccia[1], Pier Lorenzo Solari[2], Danil E. Smiles[3], David K. Shuh[3], Catherine Berthomieu[4], Didier Marcellin[4], Nicolas Bremond[4], Luisa Mangialajo[5,6], Sophie Pagnotta[8], Marguerite Monfort[7], Christophe Moulin[7], Christophe Den Auwer[1]

(1) *Université Côte d'Azur, CNRS, Institut de Chimie de Nice, UMR 7272, 06108 Nice, France*
(2) *Synchrotron Soleil, L'Orme des Merisiers, Saint-Aubin, BP 48, F-91192 Gif-sur-Yvette Cedex, France*
(3) *Chemical Sciences Division, Lawrence Berkeley National Laboratory, Berkeley, California 94720, USA*
(4) *CEA, CNRS, Aix Marseille University, BIAM UMR7265, Saint Paul-Lez-Durance, France*
(5) *Université Côte d'Azur, Université Nice Sophia Antipolis, CNRS, FRE 3729 ECOMERS, 06108 Nice, France*
(6) *Sorbonne Universités, UPMC Univ. Paris 06, INSU-CNRS, Laboratoire d'Océanographie de Villefranche, Villefranche sur mer, France*
(7) *CEA, DAM, DIF, F-92297 Arpajon, France*
(8) *Université Côte d'Azur, Centre Commun de Microscopie Appliquée, 06108 Nice France*

Abstract

Uranium speciation and bioaccumulation were investigated in the sea urchin *Paracentrotus lividus*. Through accumulation experiments in a well-controlled aquarium followed by ICP-OES analysis, the quantification of uranium in the different compartments of the sea urchin was performed. Uranium is mainly distributed in the test (skeletal components), as it is the major constituent of the sea urchin, but in terms of quantity of uranium per gram of compartment, the following rating: intestinal tract > gonads >> test, was obtained. Combining both extended X-ray Absorption Spectroscopy (XAS) and time resolved laser induced fluorescence (TRLFS) spectroscopic analysis, it was possible to identify two different forms of uranium in the sea urchin, one in the test, as a carbonato-calcium complex, and the second one in the gonads and intestinal tract, as a protein complex. Toposome is a major calcium-binding transferrin–like protein contained within the sea urchin. EXAFS data fitting of both contaminated organs *in vivo* and the uranium-toposome complex from protein purified out of the gonads revealed that it is suspected to complex uranium

in gonads and intestinal tract. This hypothesis is also supported by the results from two imaging techniques *i.e.* Transmission Electron Microscopy (TEM) and Scanning Transmission X-ray Microscopy (STXM). This thorough investigation of uranium uptake in sea urchin is one of the few attempts to assess the speciation in a living marine organism *in vivo*.

INTRODUCTION

Uranium is a natural radioelement present in the earth's crust under its natural isotope distribution (^{Nat}U: ^{238}U = 99.275%, ^{235}U = 0.719% and ^{234}U = 0.0057%). It is a very weak radiotoxin (^{Nat}U specific activity = 25767 Bq/g) but most importantly, a chemical toxin, as it is able to interact with various biological targets resulting in heavy metal poisoning. Its crustal concentration ranges between 0.3 and 12 mg/kg, depending on the geological composition. Due to anthropogenic activities, uranium is also present in the environment as technologically enhanced naturally occurring radioactive materials (TENORM) where mining activities are or have been implemented, mostly for nuclear fuel applications. Additional anthropogenic origins of uranium in the environment may also result from nuclear power accidents and nuclear weapons activities.[1-3] Last, in some particular areas of military conflict, the use of depleted uranium in munition components has resulted in the dispersion of uranium metal into the environment.[4] Most importantly, because uranium is a limited issue of public health to date (except in some specific mining or contaminated zones as mentioned above), it serves as a model (uranium is easy to manipulate in the laboratory) for more radioactive actinyls of the early actinide family, *i.e.*, neptunyl and plutonyl, predominantly in pentavalent oxidation state (+V) or, in specific oxidative conditions, as hexavalent (+VI).

In most environmental and biological conditions, uranium mainly occurs in its hexavalent oxidation state, in the form of the di-oxo uranyl cation $\{UO_2^{2+}\}$. Uranyl, if bioavailable, may compete with essential biological metal cations in binding proteins, affecting all the biological processes that depend on them.[5] For example, the coordination mechanisms of uranyl with the iron binding protein transferrin has been explored several times, by Pible *et al*. in 2006 ,[6] by Vidaud *et al.*[7] in 2007, by Hemadi *et al*. in 2009,[8] and more recently by theoretical approaches by Wang *et al*.[9] It was shown that the uranyl ion can compete with iron, which could potentially lead to the internalization of uranium in the cytoplasm of cells. However, the bioavailability and potential transfer of uranyl strongly depends on its physico-chemical speciation. For instance, several studies showed that uranyl bioavailability decreases when it is bound to some inorganic ligands (e.g., phosphate, carbonate) or adsorbed on colloidal and particulate matter.[10] This is why it is essential to deeply understand its speciation in the biosphere and biocycles, to evaluate the health risk engendered on living organisms and potentially humans, through the trophic chain.

Seawater comprises the largest percentage of the hydrosphere (*ca.* 96.5 %) and covers about 71% of the earth's surface.[11] It is also the final environmental repository for contaminated waters from rivers and basins. In oceans and seas, uranium is naturally occurring at an average concentration of around 10^{-8} M although, as for the earth's crust, heterogeneities apply.[12] In 1956, Rona *et al.* reported a concentration of uranium between 3.1 and 3.5 μg/kg in sea water at different locations, *i.e.*, in the North Atlantic, the Gulf of Mexico, and in the Straits of Florida.[13] Ku *et al.* reported similar values with a mean concentration of uranium of about 3.3 μg/L.[14] Altogether uranium represents about 1% of the total radioactivity in seawater (the major contributor being ^{40}K accounting for more than 90%).[15] In seawater, the accumulation of several heavy metals in marine organisms has been widely studied at all trophic levels.[16-18] Indeed, a wide diversity of organisms has been investigated, from simple organisms like algae to more complex ones like fish. It is far beyond the scope of this introduction to make an exhaustive report on this topic. Concerning radionuclides specifically, the IAEA (International Atomic Energy Agency) has continuously updated Concentration Factor (CF) values that could be used for impact calculations.[19-20] The CF is defined as the ratio between the concentration of the element of interest in the studied organism and the concentration of the element in the surrounding medium. The IAEA reported values of CF for ^{137}Cs and ^{90}Sr in different species of the biota, from algae to fish, and evaluated the distribution inside the organism, in multiple locations in the Baltic Sea.[19] Jeffree *et al.* recently studied the accumulation and the speciation of ^{241}Am, ^{109}Cd, ^{57}Co, ^{51}Cr, ^{134}Cs, ^{54}Mn and ^{65}Zn in spotted dog fish and turbot.[21] The distribution inside the organism was determined, and even though similarities were observed between some of the elements, the distribution is still element-dependent. Recently, Maloubier *et al.* studied the bioaccumulation of ^{241}Am and ^{152}Eu in the marine sponge *Aplysina Cavernicola* and reported speciation data for europium.[22] Some recent work has also focused only on uranium. Barillet *et al.* showed that uranium is highly bioaccumulated in Zebrafish *Danio Rerio*, and also that it can affect some of the biological functions, like hepatic defences.[23] Eb-Levadoux *et al.* also showed that in Zebrafish, uranium is reprotoxic due to a potential interaction with proteins.[24] However, to the best of our knowledge, there is no other data on uranium speciation inside marine organisms, probably because of the very low concentration of this element in seawater (ppb levels), which challenges the use of spectroscopic methods for speciation assessment. Nonetheless, speciation data obtained *in vivo* are essential to shift from a large-scale descriptive approach and inventories to a well–informed biochemical mechanistic approach.

In previous work, we investigated the uranium speciation in seawater, showing that in these conditions, it is mainly present as a dicalcium uranyl tricarbonate complex, $Ca_2UO_2(CO_3)_3$.[25] This form of uranyl has already been reported in aqueous natural systems.[26] It has also been shown not to be bioavailable when it occurs in natural drinking waters.[27] In the present report, we are addressing the question of uranium

speciation upon bioaccumulation in sea urchin *Paracentrotus lividus* (Figure 1) by proceeding to *in vivo* contamination experiments in a simplified and model biotope. We chose *P. lividus* because it is widely distributed throughout the Mediterranean Sea and the north-eastern Atlantic. Moreover, *P. lividus* is often used as a biochemical indicator of local pollution because of its sedentary habits and well-known sensitivity to pollutants. It is known to accumulate heavy metals like zinc, lead, copper, iron or cadmium.[28-29] For instance, Warnau *et al.* reported the concentration of several heavy metals (Zn, Pb, Cd, Fe, Cu, Cr and Ti) in the sea grass *Posidonia oceanica* and in the sea urchin *Paracentrotus lividus*, from three different locations in the Mediterranean Sea.[30] They also measured the quantity of each studied metal in the three different compartments of the sea urchins; the test (skeleton = shell + spines), the intestinal tract, and the gonads. They reported that the metal ion accumulation changes with the body compartment. For most metal ions, accumulation is ranked in the following order: digestive tube and gonads ≥ test. This is also what was observed one year later with other elements, *i.e.*, Ag, Cs and Am.[31] Our objective here was to assess the speciation of uranium in the different compartments of *P. lividus* in order to decipher the accumulation biomechanisms. To do so, we first described the bio-distribution of uranium in the aquarium and within the sea urchin. We have then assessed the uranium speciation in the main organs of the sea urchin (test, gonads and intestinal tract) with two spectroscopic X-ray probes that are complementary, namely X-ray Absorption Spectroscopy (XAS under both XANES and EXAFS regimes) and Scanning Transmission X-ray Microscopy (STXM) elemental imaging. They have been combined with Time Resolved Laser Fluorescence Spectroscopy (TRLFS) data and Transmission Electron Microscopy (TEM) images. In a last step, the toposome protein, which is the main protein present in the sea urchin organs, was extracted and purified out of the gonads.[32] As the toposome is a transferrin like protein and is acting as a Ca reservoir for sea urchins, it should be considered as a potential candidate for uranyl binding in the gonads. The speciation of uranyl in a solution containing the purified toposome was investigated.

EXPERIMENTAL SECTION

Seawater, sea urchin collection and aquarium setup

Seawater was collected in the Mediterranean Sea at the Environmental Laboratory of the International Atomic Energy Agency (IAEA) at 30 m from the coast of Monaco, 50 m deep (43° 43’ 49” N, 7° 25’ 40”). The seawater was filtered at 0.2 µm (Whatman, GF/C grade) and sterilized by UV treatment to eliminate particles and microorganisms. Commercial silica gravel (850 g) was placed at the bottom of the aquarium filled with 10 L of seawater. The silica gel was needed to ensure the survivability of the sea urchins inside the aquarium, and played no chemical role, nor interfered significantly with the experiments. Only one sea urchin was placed in the aquarium at the same time. The aquarium was equipped with a filter and an air

pump that were turned on 7 days before placing the sea urchins inside to equilibrate the whole system. The seawater temperature was maintained at 16°C using a water-cooling system during the experiments.

Paracentrotus lividus sea urchins (Figure 1) were collected in Villefranche-sur-mer, by the Laboratoire Océanographique de Villefranche (UMR 7093, Mediterranean Sea, France) and were fed with native algae until 3 days before contamination. The food was then removed from the aquarium, and the water was cleaned of any remnants before the first uranium spike. Specimens with similar size were chosen (average diameter = 7-8 cm, average total dry mass = 20 g). All results reported in this work concern experiments performed on female specimens. Each specimen used in this report is described in Table S1 of Supplementary Information (SI) file.

Spiking procedure and uranium distribution

Uranium nitrate $UO_2(NO_3).5H_2O$ was directly dissolved in diluted nitric acid (0.1 M) to obtain the 0.375 M uranium solution spike for aquarium use. Both nitric acid and uranium nitrate were of reagent grade, and deionized water was used to dilute the nitric acid. Every 24 hours, 500 µL of this solution were introduced in the aquarium, to reach a theoretical final concentration of $[U] = 1.88.10^{-4}$ M after 10 days. Prior to the spiking (around 10 min before), 500 µL of a 2.10^{-4} M solution of sodium hydroxide were introduced in the aquarium to avoid any modification of the pH. The latter was controlled using commercial pH paper designed for seawater. The measured pH was around 8. The uranium concentration corresponds to a total mass of uranium of 476.20 ± 27.12 mg. It was chosen as the best compromise between uranium natural concentration and EXAFS sensitivity.

Each sample from the aquarium (sea urchin or gravel) was rinsed with deionized water before any further analysis, to remove any uranium potentially adsorbed on the sample surface, and of remnant contaminated sea water, to ensure the validity of the results. The uranium content of each sample was analyzed by ICP-OES (details are provided in SI file).

Toposome extraction and purification.

The toposome purification was performed according to Castellano *et al.* with slight modifications (details are provided in SI file).[33]. The final concentration was estimated via UV-visible, using a calculated epsilon, to be around 35 mg/mL (ε = 1.252), corresponding to a molar concentration in monomer units of about 2.10^{-4} M. The epsilon was calculated using the sequence of amino acids published by Noll *et al.*[34] The toposome was then frozen until further use. The protein purity is estimated to be 80% minimum. The toposome is probably organized in the form of trimers. The two discernible fractions under the main band probably correspond to the presence of the two isoforms described at 200 kDa and 180 kDa for the *Paracentrotus lividus* toposome, which are present in the nutritive phagocytes of the gonads.[35]

Time Resolved Laser Induced Fluorescence spectroscopy (TRLFS)

Sample preparation, sea urchin: The test was dried, then crushed into powder. The powder was directly analyzed with no further preparation. Concerning the gonads, they were dried and also directly analyzed with no further preparation.

Sample preparation, toposome-uranium complex: The same procedure as described above was used. However, the uranium was this time dissolved in a solution of Tris/HCl (10mM) NaCl (10mM), pH 5.5, to reduce the ionic strength of the solution (Cl concentration). The solution was then kept at 4°C until analysis.

Data acquisition: A Nd-YAG laser (Model Surelite Quantel) operating at 355 nm (tripled) and delivering about 10 mJ of energy in a 10 ns pulse with a repetition rate of 10 Hz, was used as the excitation source. The laser output energy was monitored by a laser power meter (Scientech). The focused output beam was directed onto the urchin part (gonad, shell) of the sea urchin (previously crushed) placed in a 1 mm pathlength quartz cell of the spectrofluorometer (F900 Edinburgh). The detection was performed by an intensified charge coupled device (Andor Technology) cooled by Peltier effect (-5°C) and positioned at the polychromator exit for the emission spectra measurement and by a photomultiplier tube (PMT) to measure fluorescence decay time. Logic circuits, synchronized with the laser shot beam, allowed the intensifier to be activated with determined time delay (from 0.005 to 1000 μs) and during a determined aperture time (from 0.005 to 1000 μs). From a spectroscopic point of view, various gate delays and durations were used to ensure the presence of only one complex by the measurement of a single fluorescence lifetime and spectrum. Fluorescence lifetime measurements were performed by varying the temporal delay with fixed gate width.

X-ray Absorption Spectroscopy (XAS) Data Acquisition and Analysis

Sample preparation, sea urchins: sea urchins 2, 3 and 5 were analyzed by XAS: gonads and intestinal tract for sea urchin 2 (EXAFS), only gonads for sea urchin 3 (EXAFS) and test for sea urchin 5 (X-ray absorption near edge structure (XANES) (see Table S1). For sea urchin 2, gonads and intestinal tract were freeze-dried for 24h. Solid pellets were then prepared by mixing the dry residue with polyethylene in order to obtain homogenous solid pellets. For sea urchin 3, solid pellets were prepared with the gonads by mixing fresh gonads with polyethylene. As polyethylene is only composed of light chemical elements, it does not interfere with the EXAFS measurements. In both cases, the pellets were then kept at -20°C until the analysis to avoid any deterioration of the biological system. For sea urchin 5, the test was mechanically ground and pressed into solid pellets. The Liebigite reference sample ($Ca_2UO_2(CO_3)_3$) was obtained from the mineralogy collection of the Museum National d'Histoire Naturelle (MNHN), Paris, France.

Sample preparation, U-toposome complex: uranium nitrate was directly dissolved in Tris/HCl (50mM) NaCl (150mM), pH = 5.5. This pH value prevents any visible precipitation of uranium hydroxides. Absence

of hydrolysis was also verified using speciation codes. pH was adjusted to 5.5 with concentrated chlorhydric acid. The solution was then mixed with the protein, to obtain a final concentration of uranium of 8.10^{-5} M, and a concentration of protein in monomeric units estimated at 1.6. 10^{-4} M. An estimated excess of protein ensures that no free uranyl would remain in the solution, which would interfere with the EXAFS analysis. The solution was then kept at 4°C until analysis.

EXAFS data acquisition: experiments were performed on the MARS beamline of the SOLEIL synchrotron facility. Energy calibration was performed at the yttrium K edge at 17038 eV and EXAFS experiments at the U L_{III} edge. The MARS beamline is dedicated to the investigation of radioactive materials in the hard X-ray range.[36] The beamline optics consist essentially of a water-cooled double-crystal monochromator (FMB Oxford), which is used to select the incident energy of the X-ray beam and for horizontal focalization, and two large water-cooled reflecting mirrors (IRELEC/SESO) that are used for high-energy rejection (harmonic part) and vertical collimation and focalization. All measurements were achieved in fluorescence mode using a 13-element high purity germanium detector (ORTEC). The X-ray absorption spectra for the test sample (from sea urchin 5) were measured at room temperature, whereas the spectra for the gonad samples (from sea urchins 2 and 3) and for the intestinal tract sample (from sea urchin 3) were measured at -165 °C. To perform the latter measurements, the samples were inserted in a specifically designed double containment cell (H. Hermange, SOLEIL) and inserted in the dedicated liquid nitrogen cryostat of the beamline. The protein sample was measured at room temperature.

EXAFS data processing was performed using the ATHENA code.[37-38] The E_0 energy was identified at the maximum of the absorption edge. Fourier transform (FT) with k^2 weighting was performed between 2.5 and 12 $Å^{-1}$ for gonads and 10.5 $Å^{-1}$ for the intestinal tract, with a Hanning window. The fits were performed using the DEMETER code (version Demeter 0.9.25) and were fit in R space between 1 and 5 Å. EXAFS data fitting: One global amplitude factor S_0^2 and one energy threshold correction factor ΔE_0 were used for every path of the fits. The agreement factor r (%) and the quality factor (QF = reduced χ^2) of the fits were provided directly by DEMETER. Phases and amplitudes were calculated using the FEFF6 simulation code integrated in DEMETER based on a partial structural model (*in silico*) of uranyl-acetate complex ($UO_2(acetate)_2$.) This model was chosen because it exhibits both monodentate and bidentate carboxylate ligation to the uranyl equatorial plane. The scattering paths used for the fitting procedure are: i) simple scattering paths including U-O_{ax} within the oxo bond, U-O_{eq} corresponding to the equatorial oxygen atoms and U...C corresponding to the C atom of the bidentate carboxylate group; ii) multiple scattering paths including the quadruple path U-O_{ax} within the oxo bond, and the triple scattering U-O-C of the monodentate carboxylate function. During the fitting procedure, the number of atoms of carbon in the monodentate and bidentate functions was let free, in case only one coordination mode was present. The total number of variables in the fit was equal to 12.

Transmission electron microscope (TEM) imaging

Gonads and intestinal tract of sea urchin 2 were analysed with TEM. Directly after dissection, fresh gonads and fresh intestinal tract samples were fixed for 2 h at room temperature with 2.5% glutaraldehyde in cacodylate buffer (0.1 M, pH 7.4) in artificial seawater, then washed with 0.1 M cacodylate buffer (pH 7.4) and post-fixed with 1 % osmium tetroxide in cacodylate buffer containing 1% potassium ferrocyanide. The samples were embedded in Epon resin after dehydration using an acetone/water solution and then acetone. Ultrathin sections (70–80 nm) were cut using a diamond diatom mounted on an ultramicrotome (Ultracut S, Leica) and placed on copper TEM grids coated with formvar film. Sections were observed with a JEOL JEM 1400 TEM equipped with a CCD camera (Morada, Olympus SIS) at the Centre for Applied Microscopy (CCMA, University of Nice Sophia Antipolis, Nice, France).

Scanning transmission X-ray microscope (STXM) imaging

Sample preparation: Gonad and intestinal tract cells of sea urchin 2 were analysed with STXM. The STXM samples were prepared as described above for TEM analysis. Sections of 70-80 nm were placed on a 100 nm thick Si_3N_4 membrane window (1 mm square) in a 10 mm frame obtained from Silson Ltd. A second Si_3N_4 window was glued over the first to seal and confine the sample for radiological control purposes.

Data acquisition: Data was recorded with the STXM on beamline 11.0.2 of the Advanced Light Source (ALS) located at the Lawrence Berkeley National Laboratory in Berkeley, USA.[39] The STXM methodology employed in this study was similar to that described previously.[40-41] The photon energy calibration of the monochromator was performed at the neon K-edge (867.3 eV). The STXM measurements were performed with a 25 nm zone plate in transmission mode and the ALS was operating in top-off mode with a beam current of 500 mA. Images at a single energy were obtained by raster scanning the sample and collecting X-rays as a function of sample position. Elemental maps of uranium were obtained by subtracting an image taken before the absorption threshold from an image obtained at resonance utilizing the U N_5 transition (~738 eV), following image alignment.

Data treatment: Data treatment was performed with the aXis2000 code developed at McMaster University.[42]

RESULTS AND DISCUSSION

Uranium uptake and distribution in the organs.

We have investigated the uptake of uranium by *P. lividus* in the closed aquarium system described in the experimental section (1 spike per day for 10 days). Four similar experiments have been conducted with five

sea urchins that are detailed in Table S1. A control experiment with no spike was also performed at the same time in a similar aquarium next to the one used for contamination. It showed that no detectable uranium was naturally present in sea urchins (below the detection limit of ICP-OES, about $1x10^{-7}$ mg/L). Each *P. lividus* specimen was sacrificed and dissected at the end of the 10 days. Gonads, digestive tube and test were separated, and uranium content was measured by ICP-OES.

First, the total uranium balance was measured in the entire system with sea urchin 4 to ensure that the major part of the uranium was distributed within the main components (sea water, gravel, sea urchin), and not, for instance, adsorbed on the aquarium wall or filter. The concentration of uranium in each of the different system components was measured. The results are presented in Figure S1. From the concentration in seawater, the global Concentration Factor (CF) of sea urchin 4 for an exposure of 10 days was calculated and is 0.37±0.02.

The bioaccumulation of uranium in each compartment of the sea urchin (test, gonad, intestinal tract) has been assessed. Although competition between uranium and other cations was not explicitly taken into account, the use of a natural medium implies that competition is implicitly included. It is presented in Figure 2 for sea urchins 1, 2 and 4 as the fraction of total uranium mass per dry weight of each compartment (see Table S2). In the three specimens, the concentration in the digestive tube is almost 3 times and 10 times higher than in the gonads and test, respectively. Differences can be observed between sea urchin 4 and the two others. We explain these discrepancies by the seasonal variations in the gonads quantity and the seasonal variations in the concentration of proteins inside the gonads. Indeed, the experiment on sea urchin 4 was conducted out of the reproduction season (February-May), which was not the case for sea urchins 1 and 2. Partial concentration factors for each compartment may also be calculated. The following CF were obtained for sea urchin 1: CF_{gonads} = 1.0±0.07, $CF_{intestin}$ = 2.8±0.1 and CF_{test} = 0.25±0.02. The overall very low value obtained for the entire specimen is largely due to the low value of CF_{test} that is associated to the largest mass of the specimen (the test). These results are in agreement with the values reported by Warnau *et al.* in 1996 as the same ordering was observed for most heavy metals: gonads, intestinal tract >> test. In their communication, the concentration measured in the intestinal tract is the highest of the three compartments for several heavy metals as iron, copper, tin and mercury. However, the gonads are more concentrated in zinc than the intestinal tract, which means that the distribution is element specific and also confirms that speciation is playing a key role in the accumulation mechanisms. In addition, Warnau *et al.* also highlighted the fact that the concentrations of every metal but lead are always lower in the test than the gonads or the intestinal tract, no matter which of the two latter compartments is the most concentrated. These data clearly highlight the necessity of speciation investigation in each compartment separately, as the accumulation rate of uranium is radically different between the three compartments.

Uranium speciation in the test

The test of sea urchin is mainly composed of monocrystalline calcite (calcium carbonate) rich in magnesium.[43] Uranium accumulation in test and spines is very low, as mentioned above, with an average concentration of 11 ppm (CF_{test} = 0.25±0.02). Such a concentration lies just above the estimated EXAFS detection limit under our experimental conditions. Therefore, an EXAFS spectrum could not be recorded from the test with a reasonable signal to noise ratio and only the XANES part of the spectrum was significant. Figure 3 compares the XANES spectra of the test after *in vivo* contamination of sea urchin 5 with data acquired from a Liebigite ($Ca_2UO_2(CO_3)_3$) solid state reference. Liebigite is taken here as the model for the main species of uranium in seawater, the dicalcic uranyl tricarbonate species, $Ca_2UO_2(CO_3)_3$. The enlarged insert of Figure 3 shows the derivatives of the spectra. A qualitative comparison of both XANES spectra and their derivatives for the test samples and the Liebigite reference suggests that the speciation of uranium in the test is similar to that in the Liebigite model, although it is not definite proof. This could signify that a sorption mechanism occurs and is at the origin of the uranium accumulation in the test. As adult spines do not grow once they reach their adult size, a mechanism involving sorption on the calcite monocrystalline surface of the spines followed by slow diffusion of uranium inside the calcite structure agrees well with the final very low concentration of uranium in the test, contrary to a mechanism of incorporation of the uranium during the growth of the spines. To complement the XANES results, TRLFS measurements were also performed on sea urchin 5. The wavelengths of the maximum of fluorescence emissions obtained are 471, 488, 507, 528 and 552 nm (Figure 4). Previous studies on uranium compounds[25] report the wavelengths obtained for different species, including uranium in seawater, several carbonated calcium-uranium complexes, and sulphate and phosphate uranium complexes. Indeed, a slight hypsochromic shift is noticed here, mainly for the higher wavelengths compared to free uranyl (reported wavelengths: 470–488–509–534–559 nm), which is characteristic of M_x–UO_2–$(CO_3)_y$ complexes (with x : 1-2 and y : 2-3), with M = Ca^{2+}, Mg^{2+} and Sr^{2+}.

Even though it is not possible to differentiate all the possible species, the results above are consistent with the presence of the dicalcic uranyl tricarbonate species in the test at a relatively low level.

Uranium accumulation in the gonad and intestinal tract cells, imaging and spectroscopy

Transmission electron microscope (TEM) imaging was performed on the gonad cells of contaminated sea urchin 2. Figure 5 shows a large field TEM image of the gonads. More specifically, two types of cells can be observed; the reproductive cells (circular and darker), and the storage cells (various shapes, lighter). No evidence of uranium precipitates can be noted on this micrograph in any of the cells although uranium is present in the gonads at a concentration of around 50 ppm, as mentioned before. Precipitates of uranium phosphate phases have been observed for different bacterial systems. For instance, Suzuki *et al.* reported

that nanoprecipitates of uranium were visible extra-cellularly in *Deinococcus radiodurans* after exposure.[44] Uranium-phosphate crystals were also reported to be present inside cells of *Stenotrophomonas Maltophilia* by Merroun *et al.*[45] It was also observed in living cells UMR-106, which are model osteoblastic cells.[46] The absence of any visible precipitate, although not a definite proof, suggests that uranyl is not incorporated as an insoluble mineral phase. To further investigate this assumption, STXM elemental imaging was performed on gonads cells of the same sea urchin specimen. Figure 6 shows the STXM image recorded at 738 eV, just above the uranium N_V edge. One can clearly distinguish the cell membrane and the different organelles inside. The elemental map was then obtained *via* alignment and subtraction of the STXM image collected at an energy preceeding the N_V edge at 725 eV (Figure S5). The elemental map reveals a featureless map with a shadow ring at the location of the cell wall although the contrast in the shadow ring is noticeable but only 2% above background. Thus, the elemental map shows that uranium is not localized in specific hot spots or precipitates to our degree of both spatial and spectral resolution but may be homogeneously distributed around the cell membrane. As a consequence, both TEM and STXM images suggest that uranium may be complexed within the cell by proteins, enzyme or metabolites even though this is clearly not a definitive evidence because only a limited number of cells were observed and the signal of the shadow ring in the uranium elemental map is very weak.

Considering the affinity of uranyl for hard donor oxygen groups like in the transferrin binding site (aspartate, tyrosine, carbonate)[7,47], complexation of the uranyl cation by carboxylate rich proteins, enzyme or metabolites is a reasonable assumption. This could also explain the low contrast observed in the STXM contrast image because it would be distributed over the entire cell membrane. Such ligation could involve aspartic, glutamic or tyrosine residues, for instance. To further determine the speciation of uranium inside the cells and possible complexation, contaminated gonads of sea urchin 2 and 3 were analysed by EXAFS and XANES spectroscopy at the uranium L_{III} edge. The XANES spectrum of the gonads of sea urchin 2 is provided in Figure 3 and exhibits the expected uranyl pattern. The EXAFS spectra obtained for the gonades of sea urchins 2 and 3 are presented in Figure 7. The experimental spectrum for sea urchin 2 was adjusted with a model composed of 3 scattering shells (O_{yle}, O_{eq} and C) as explained in the experimental section (the spectrum corresponding to sea urchin 3 being superimposable, but at lower signal to noise ratio, is shown but not fitted). The best fit metrical parameters are reported in Table 1, the Fourier transform (modulus and imaginary parts) is provided in Figure S6. The first shell corresponds to the two axial oxygen atoms typical of the uranyl oxocation. The second shell is composed of 5.1(3) O atoms at 2.37(1) Å (average) and the last shell is composed of 3.3(9) C atoms at 2.94(3) Å. Such a coordination sphere is indeed typical of carboxylate rich biomolecules, although a detailed path by path analysis is not possible here in the absence of a specific structural model. Alternative attempts to fit our data with a Liebigite model lead to unrealistic metrical parameters, thus supporting protein or metabolite complexation. Pible *et al.* in 2006 studied the interaction

between uranyl and a wide number of proteins.[6] They calculated and reported the distances between uranium and selected protein structures containing uranyl. Values for the U-O_{eq} distances fall into the range 2.31 - 2.61 Å for monodentate carboxylate groups and 2.41 - 2.84 Å for bidentate carboxylate groups. In the specific case of transferrin, Hémadi *et al.* in 2009 and Wang *et al.* more recently reported the binding mechanism of uranyl to transferrin by DFT calculations.[8-9] In the model of Wang, the most probable coordination sphere is composed of one bidentate carbonate with U-O at 2.46 Å, two tyrosines with U-O at 2.30 Å, and one monodentate aspartate at a distance of 2.44 Å. The values we obtained for the U-O_{eq} average distance (reported in Table 1) seems to indicate the presence of monodentate carboxylate groups although only average values are discussed here. Concerning the carbons atoms, the U...C average distances reported in Table 1 in the range 2.9 - 3.0 Å also support the presence of bidentate carboxylate functions. No evidence of monodentate complexation was found using the U...C interaction. However, this is not an absolute proof, considering that this interaction is often very weak, due to the angle of the U-O-C bond (deviating from focusing effect optimum angle, 180°) in monodentate configuration. On the other hand, the triple scattering path U-C-O was found to be necessary to fit the experimental data. This path being a fingerprint of monodentate ligation, it suggests the occurrence of at least one monodentate carboxylate function. We thus propose here the following mode of coordination: two atoms of oxygen (for the oxo bonds), a mix of monodentate and bidentate carboxylate functions with an unknown ratio, and possibly one water molecule to complement the equatorial coordination sphere. The above structural data therefore suggest that uranyl is coordinated to carboxylate residues of a protein or metabolite.

As for the gonad cells, the EXAFS (Figure 7) and XANES (Figure 3) spectra at the L_{III} edge of uranium was recorded for the intestinal tract cells of sea urchin 2. Qualitatively, the spectra are very similar to what is discussed above, suggesting that the same type of complexation occurs in this compartment as well. Experimental and simulated EXAFS spectra are displayed in Figure 7, best fit structural parameters are also reported in Table 1. The U-O_{eq} average distance (2.35(1) Å) is similar to those obtained for the gonad cells (2.37(1) Å) and the same type of U...C path has been used. This suggests that the same biomolecule (or same type) is involved in the uranium complexation in the intestinal tract.

In addition, TRFLS measurements were also performed (Figure 4) on the gonads of sea urchin 5. The following fluorescence wavelengths were obtained: 501-521-542 nm. In contrast to what was obtained for the test, a bathochromic effect with respect to free uranyl (488–509–534 nm) is observed, together with two lifetimes of 140 µs and 1600 µs without modification of the spectra. This indicates that the carbonato calcite form of uranyl is not the correct speciation within the gonads, as already supported by the EXAFS data fitting. Bathochromic effects have been reported to occur in the presence of complexing ligands, such as sulphate or phosphonate, the latter leading to the largest shift (main wavelengths: 496-519-545). In the present case, the shift is even more important taken together with the broadening of the spectrum, indicating

that most of the uranyl is likely to be complexed with a strong complexing ligand with multiple interaction sites such as macromolecules that establish several local environments (and account for the broadening observed as well as the different lifetimes).

In conclusion, the best fit EXAFS data support the hypothesis of a complexation of the uranyl with carboxylate rich proteins, enzymes or metabolites in gonads and intestinal tract cells. This assumption is also in full agreement with both STXM and TEM imaging.

Uranium-toposome complexation

The toposome is the main protein in sea urchins and is present in both the gonads and intestinal tract. It is described as a multimer of 180 kDa monomers, known as 22S fragment.[48]

This protein, also referred to as major yolk protein, was previously identified as a calcium binding iron-less transferrin like protein.[35] As a consequence, toposome is a potential candidate for uranyl complexation in the cells. Different final masses are reported, depending on the number of monomers (from 1 to 6). As a consequence, toposome is a potential candidate for uranyl complexation in the cells.

Following toposome extraction from gonad cells and purification, the EXAFS spectrum at the L_{III} edge of uranium was recorded for the U-toposome complex in solution. The experimental XANES data, the experimental EXAFS spectra and the best simulated EXAFS spectra are similar to both gonads and intestinal tract spectra although some slight differences appear between 6 and 9 $Å^{-1}$ (Figure 7). Nonetheless, the similarities between the best fit structural parameters (reported in Table 1) obtained for the three systems strongly suggest that the toposome protein is a good match for uranyl complexation in those two compartments. The slight differences observed in the EXAFS spectra, notably in the wave between 6 and 9 $Å^{-1}$ are not due to differences in the nature of the binding site (like carboxylate *versus* phosphate ligation for instance) but most probably to differences in conformation as indicated by the similarities of the imaginary parts of the moduli of the FT (Figure S6).

TRFLS measurements were also performed on a U-toposome solution (2:1 ratio, $[UO_2]$ = 1μM). The spectrum represented in Figure 4 exhibits the same fluorescence wavelengths as observed before (501-521-542nm). However, two other fluorescence wavelengths must be highlighted: 485nm and 465nm, the latter being characteristic of carboxylic functions. This validates the EXAFS interpretation for the U-toposome complex and suggests that the speciation of uranyl in the toposome complex and in gonads and intestinal tract cells is similar. The absence of the 465 nm wavelength in the gonad TRLFS spectrum may be explained because the gonads are not only composed of toposome, even though it is the main protein. Other proteins or metabolites and thus other complexation conformations might be present. The spectrum obtained for gonads is in consequence less specific.

The fact that the toposome is likely to complex uranyl inside the sea urchin is a result of great interest, as it is a strong evidence of the metabolization of uranyl inside a living organism, from a dicalcic carbonato form in seawater to a protein complex inside the sea urchin. This shows the importance of speciation as a key parameter to understand and evaluate the potential impact on the environment and on humans that this element, and by extension, other similar elements, can have, if released in the environment. There is still an important need to continue these studies, as the speciation of multiple radioisotopes in biocycles remains completely unknown.

Associated content

The Supporting Information is available free of charge on the ACS Publications website at …

The SI contains Table S1, which describes the different measurements on the 5 sea urchins. Results dealing about the distribution of the uranium inside the sea urchin organs and inside the aquarium (Table S2 and Figure S1). Elution profiles and SDS gel are presented Figure S2, S3 and S4. Complementary STXM images and EXAFS data are also presented (Figure S5 and S6).

Author information

Corresponding author:

*C. Den Auwer, Phone: +0033 , E-mail : christophe.denauwer@univ-cotedazur.fr

The authors declare no competing financial interest.

ACKNOWLEDGMENTS:

This work was financed by the DNP (Direction of Nuclear Propulsion) of CEA DAM. We thank the International Atomic Energy Agency, Environmental Laboratory of Monaco for providing the seawater. We also acknowledge the LOV, UMR 7093 for providing the sea urchins and the algae. The XAS experiments were performed at the MARS beamline of the SOLEIL synchrotron facility, Gif sur Yvette, France. This research was supported in part (DES, DKS) by the Director, Office of Science, Office of Basic Energy Sciences, Division of Chemical Sciences, Geosciences, and Biosciences Heavy Elements Chemistry program of the U.S. Department of Energy under Contract Number DE-AC02-05CH11231 at Lawrence Berkeley National Laboratory (LBNL). This research used resources of the Advanced Light Source, which is a U.S. Department of Energy Office of Science User Facility supported under Contract No. DE-AC02-05CH11231 at LBNL. Finally, we thank the Centre Commun de Microscopie Appliquée for the SEM imaging.

Table 1: Best fit parameters for EXAFS data from the U L_{III} edge. Numbers in brackets are the estimated uncertainties, numbers in italics have been fixed. σ^2 is the Debye Waller factor of the considered scattering path. S_0^2 is the global amplitude factor, e_0 is the energy threshold, R_{factor} is the agreement factor of the fit in % and Q is the quality factor (reduced CHI^2) of the fit.

Sea urchin 2	First coordination shell	Second coordination shell	Third coordination shell	Fit parameters[a]
Gonads	2 O_{ax} at 1.79 (1) Å, σ^2 = 0.003 Å^2	5.1 (3) O_{eq} at 2.37 (1) Å, σ^2 = 0.008 Å^2	3.3 (9) C at 2.94 (3) Å σ^2 = 0.007 Å^2	*S_0^2 = 1.00* e_0 = 1.56 eV R_{factor} = 1.6 % Q = 2
Intestinal tract	2 O_{ax} at 1.79 (1) Å, σ^2 = 0.007 Å^2	5.8 (8) Oeq at 2.34 (1) Å, σ^2 = 0.010 Å^2	3.8 (7) C at 2.96 (5) Å, σ^2 = 0.001 Å^2	*S_0^2 = 1.00* e_0 = 3.34 eV R_{factor} = 2.2 % Q = 4
Toposome	2 O_{ax} at 1.78 (1) Å, σ^2 = 0.003 Å^2	5.5 (9) Oeq at 2.35 (2) Å σ^2 = 0.011 Å^2	3.4 (7) C at 2.89 (3) Å σ^2 = 0.001 Å^2	*S_0^2 = 1.10* e_0 = 3.29 eV R_{factor} = 2.2 % Q = 12

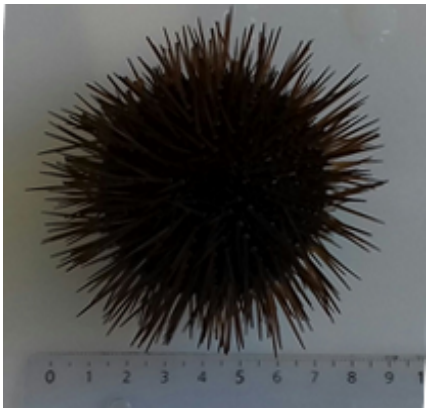

Figure 1: Picture of a sea urchin *Paracentrotus lividus* (one unit = one centimeter).

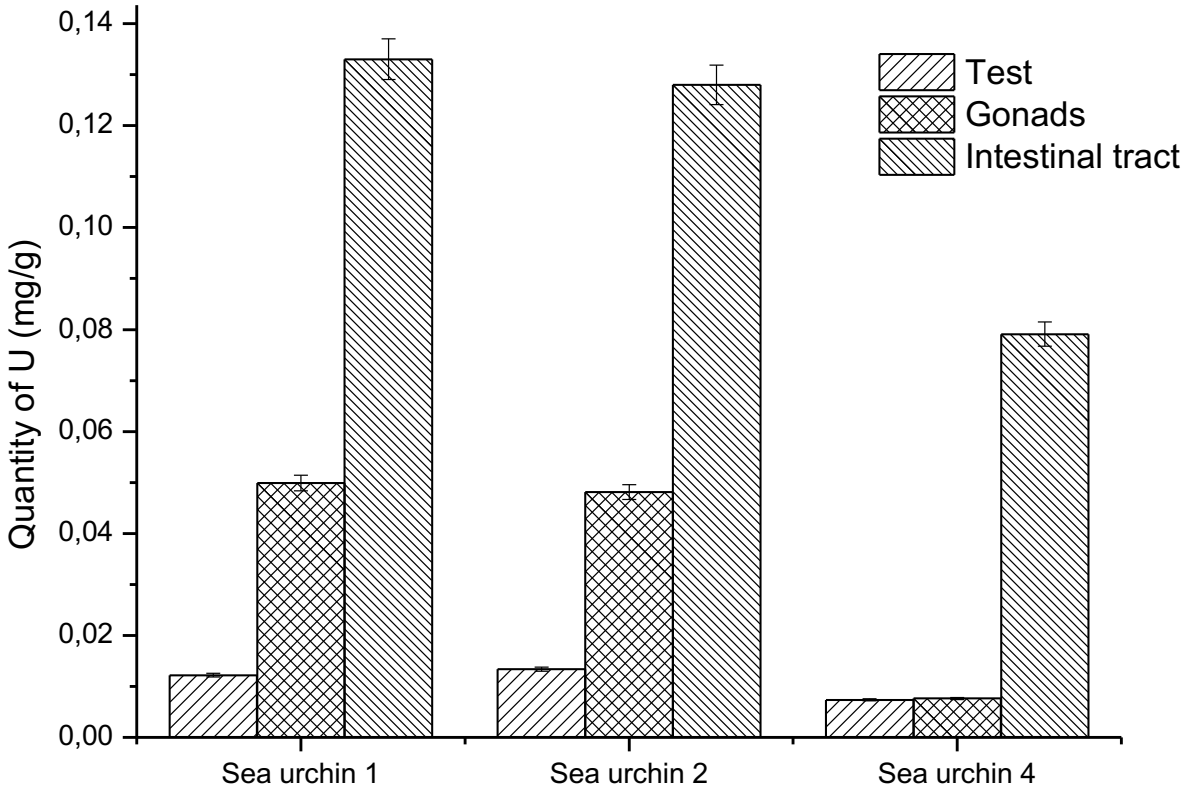

Figure 2: Uranium concentration (in mg/g, elemental U) for the three compartments of the sea urchins 1, 2 and 4.

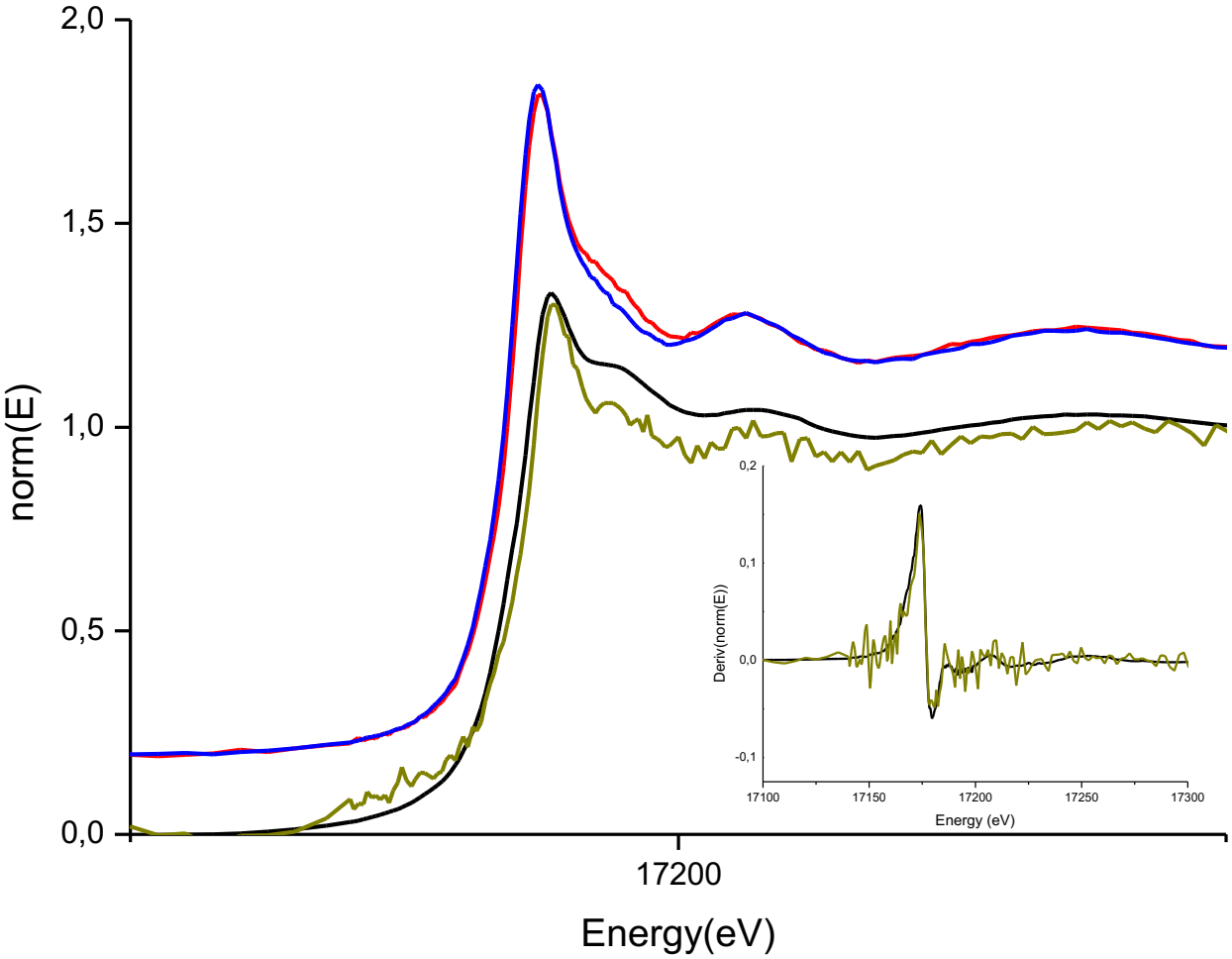

Figure 3: XANES spectra at the U LIII edge of the test of sea urchin 5 (green), of the Liebigite reference sample (black), of the gonads (red) and the intestinal tract (blue) of sea urchin 2 (both shifted in ordinates for clarity). Insert: Enlargement of the corresponding first derivatives of the test and the Liebigite reference sample.

506

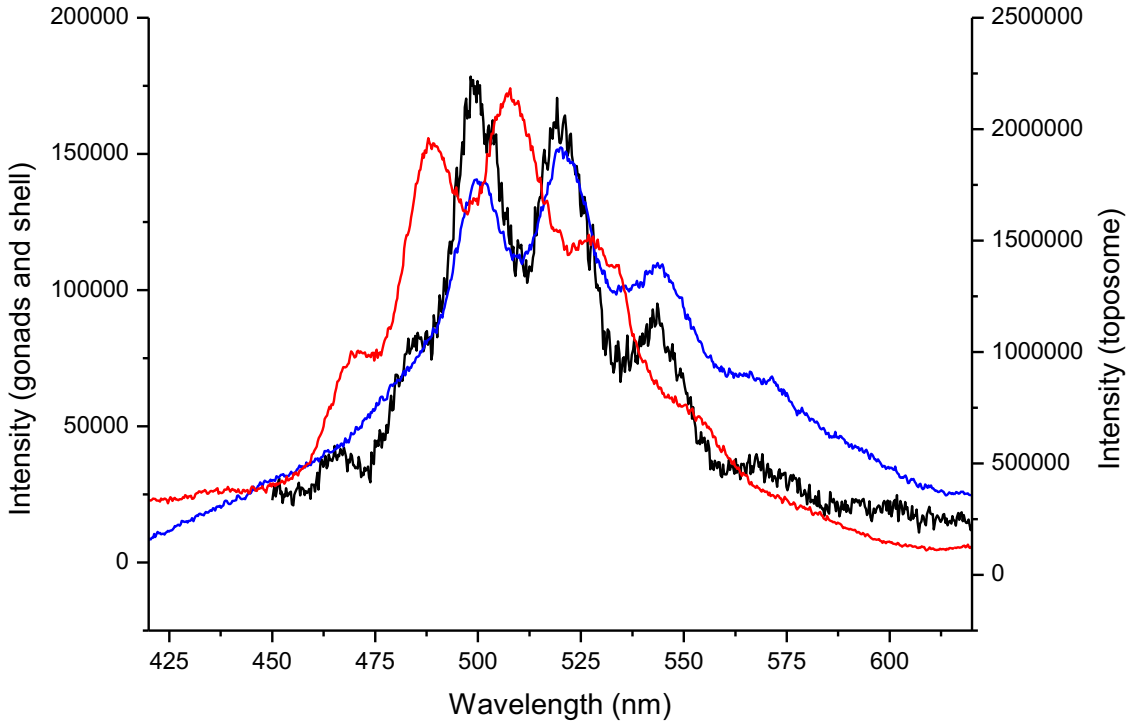

Figure 4: TRFLS spectra obtained for the contaminated test of sea urchin 5 (red), for the contaminated gonads of sea urchin 5 (blue) and U-toposome complex (black)

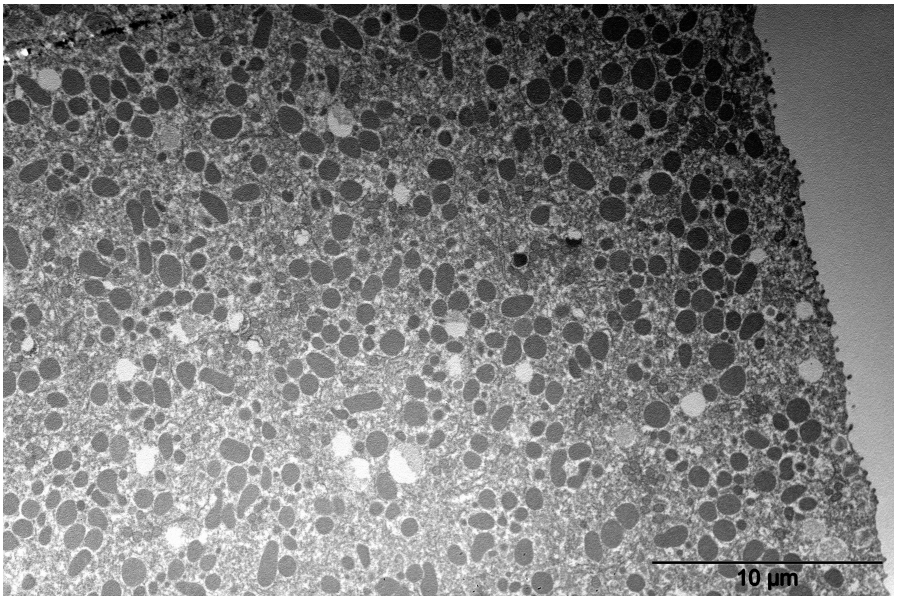

Figure 5: TEM imaging performed on the gonads of sea urchin 2.

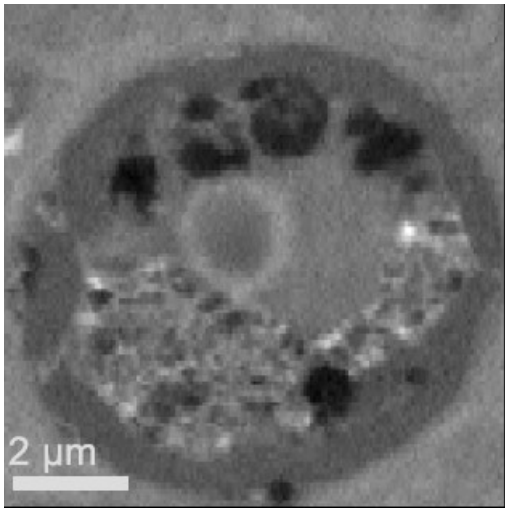

Figure 6: STXM normal contrast image of the sea urchin 2 gonad cells collected at 738 eV.

514
515
516
517
518
519

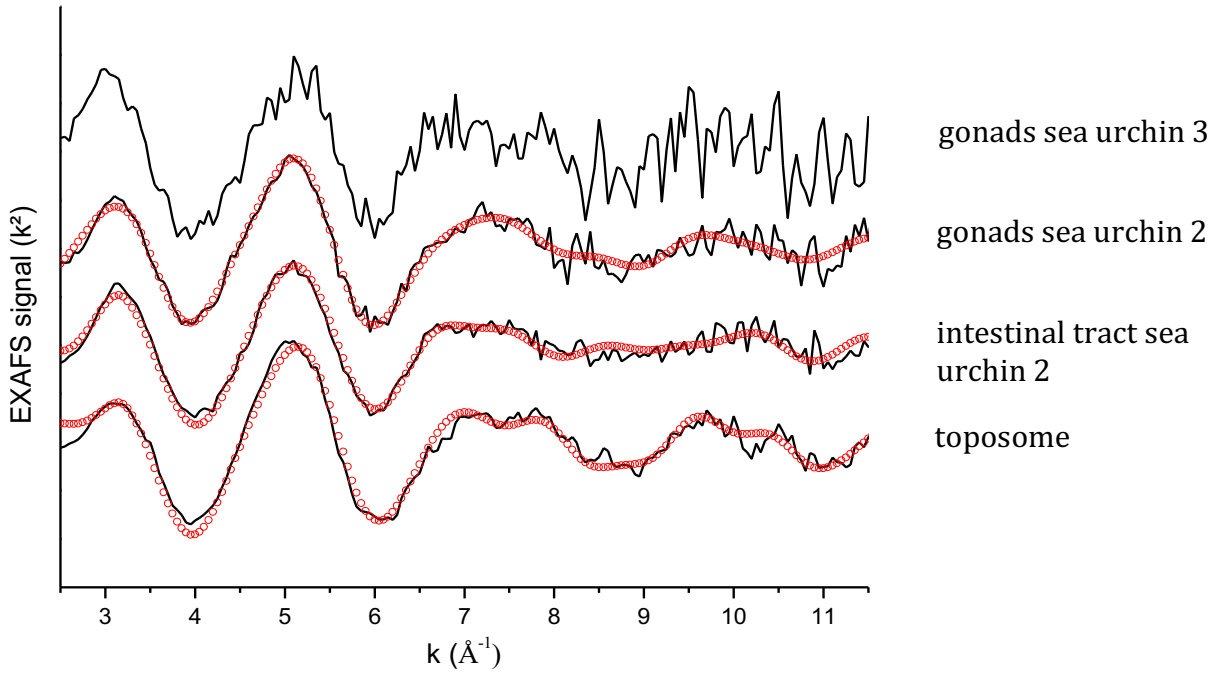

Figure 7 : EXAFS spectra (k^2) at the U L_{III} edge of the contaminated intestinal tract of sea urchin 2 (SU2) and the U-toposome complex. The EXAFS spectra obtained for the contaminated gonads of sea urchin 3(SU3) is also presented. Experimental = straight line; fit = red dots.

References:

[1] Pereira R., Barbosa S., Carvalho F.P., Uranium mining in Portugal: a review of the environmental legacies of the largest mines and environmental and human health impacts. *Environ. Geochem. Health* **2014,** *36 (2),* 285-301.

[2] Wendel C.C., Fifield L.K., Oughton D.H., Lind O.C., Skipperud L., Bartnicki J., Tims S.G., Høibråten S., Salbu B., Long-range tropospheric transport of uranium and plutonium weapons fallout from Semipalatinsk nuclear test site to Norway. *Environ. Int*. **2013**, *59,* 92-102.

[3] Abe Y., Iizawa Y., Terada Y., Adachi K., Igarashi Y., Nakai I., Detection of uranium and chemical state analysis of individual radioactive microparticles emitted from the Fukushima nuclear accident using multiple synchrotron radiation X-ray analyses. *Anal. Chem.* **2014**, *86 (17)*, 8521-8525.

[4] Bleise A., Danesi P.R., Burkart W., Properties, use and health effects of depleted uranium (DU): a general overview. *J. Environ. Radioactiv.* **2003**, *64 (2-3)*, 93–112.

[5] Michon J., Frelon S., Garnier C., Coppin F., Determinations of Uranium (VI) Binding Properties with some Metalloproteins (Transferrin, Albumin, Metallotionein and Ferritin) by Fluorescence Quenching. *J. Fluoresc* **2010**, *20 (2)*, 581-590.

[6] Pible O., Guilbaud P., Pellequer J.-L., Vidaud C., Quéméneur E., Structural insights into protein–uranyl interaction: towards an *in-silico* detection method. *Biochimie* **2006,** *88* ,1631–1638.

[7] Vidaud C., Gourion-Arsiquaud A., Rollin-Genetet F., Torne-Celer C., Plantevin S., Pible O., Berthomieu C., Quemeneur E. Structural Consequences of Binding of UO_2^{2+} to Apotransferrin: Can This Protein Account for Entry of Uranium into Human Cells. Biochemistry **2007** *46,* 2215-2226.

[8] Hemadi M., Ha-Duong N.T., Plantevin S., Vidaud C., El Hage Chahine J.M., Can uranium follow the iron-acquisition pathway? Interaction of uranyl-loaded transferrin with receptor 1. *J. Biol. Inorg. Chem*. **2010**, *15*, 497–504.

[9] Wang M., Ding W., Wang D., Binding mechanism of uranyl to transferrin implicated by density functional theory study. *RSC Adv*. **2017**, *7*, 3667.

[10] Markich S.J., Uranium Speciation and Bioavailability in Aquatic Systems: An Overview. *TheScientificWorldJo* **2002**, *(2)*, 707-729.

[11] data from U.S. Geological Survey, www.usgs.us

[12] Chen J.H., Lawrence Edwards R., Wasserburg G.J., ^{238}U,^{234}U and^{232}Th in seawater. *Earth Planet. Sc. Lett.* **1986,** *80 (3–4)*, 241-251.

[13] Rona E., Gilpatrick L. O., Jeffrey L. M., Uranium determination in sea water. *EOS T. Am. Geophys. Un.* **1956**, *37 (6)*, 697-701.

[14] Ku T.L., Knauss K.G., Mathieu G.G., Uranium in open ocean: concentration and isotopic composition. *Deep-Sea Res.* **1977,** *24 (11)*, 1005-1010.

[15] Guegueniat, P., Germain, P., Metivier, H., Radionuclides in the oceans: inputs and inventories., **1996**, France: Les editions de physique.

[16] Soualili D., Dubois P., Gosselin P., Pernet P., Guillou M., Assessment of seawater pollution by heavy metals in the neighbourhood of Algiers: use of the sea urchin, Paracentrotus lividus, as a bioindicator. *ICES J. Mar. Sci.* **2008**, *65,* 132–139.

[17] Bernd S., The use of fish parasites as bioindicators of heavy metals in aquatic ecosystems: a review. *Aquat. Ecol.* **2001**, *35*, 245–255.

[18] Mostafa H. M., Collins K. J., Heavy metal concentrations in sea urchin tissues from Egypt, Ireland and United Kingdom. *Chem. Ecol.* **1995**, *10 (1-2)*, 181-190.

[19] INTERNATIONAL ATOMIC ENERGY AGENCY, Sediment Distribution Coefficients and Concentration Factors for Biota in the Marine Environment, *Technical Reports Series No. 247*, **1985**.

[20] INTERNATIONAL ATOMIC ENERGY AGENCY, Sediment Distribution Coefficients and Concentration Factors for Biota in the Marine Environment, *Technical Reports Series No. 422*, **2004.**

[21] Jeffree R. A., Warnau M., Teyssié J-L., Markich S. J., Comparison of the bioaccumulation from seawater and depuration of heavy metals and radionuclides in the spotted dogfish *Scyliorhinus canicula*

(Chondrichthys) and the turbot *Psetta maxima (Actinopterygii: Teleostei)*. *Sci. Total Environ.* **2006**, *368 (2-3)*, 839–852.
[22] Maloubier M., Michel H., Solari P.L., Moisy P., Tribalat M-A., Oberhaensli F.R., M-J. Dechraoui Botteine, Thomas O.P., Monfort M., Moulin C., Den Auwer C., Speciation of americium in seawater and accumulation in the marine sponge *Aplysina cavernicola. Dalton Trans*. **2015**, *44 (47)*, 20584-20596.
[23] Barillet S., Adam-Guillermin C., Palluel O., Porcher J-M., Devaux A., Uranium bioaccumulation and biological disorders induced in zebrafish (*Danio rerio*) after a depleted uranium waterborne exposure. *Environ. Pollut.* **2011,** *159 (2),* 495-502.
[24] Eb-Levadoux Y., Frelon S., Simon O., Arnaudguilhem C. Lobinski R., Mounicou S., *In vivo* identification of potential uranium protein targets in zebrafish ovaries after chronic waterborne exposure. *Metallomics* **2017**, *9 (5)***,** 525-534.
[25] Maloubier M, Solari P.L, Moisy P, Monfort M, Den Auwer C, Moulin C., XAS and TRLIF spectroscopy of uranium and neptunium in seawater. *Dalton Trans.* **2015,** *28 (12),* 5417-5427.
[26] Kelly S. D., Kemner K. M., Brooks S. C., X-ray absorption spectroscopy identifies calcium-uranyl-carbonate complexes at environmental concentrations. *Geochim. Cosmochim. Ac.* **2007,** *71 (4),* 821–834.
[27] Prat O., Vercouter T., Ansoborlo E., Fichet P., Perret P., Kurttio P., Salonen L., Uranium Speciation in Drinking Water from Drilled Wells in Southern Finland and Its Potential Links to Health Effects. *Environ. Sci. Technol.* **2009***, 43* (10), 3941-3946.
[28] Auernheimer C., Chinchon S., Calcareous skeletons of sea urchins as indicators of heavy metals pollution. Portman Bay, Spain. *Environ. Geol.* **1997**, *29 (1-2),* 78-83.
[29] Rouane-Hacene, O., Boutiba, Z., Benaissa, M., Belhaouari B., Francour P., Guibbolini-Sabatier M.E., Risso-De Faverney C., Seasonal assessment of biological indices, bioaccumulation, and bioavailability of heavy metals in sea urchins Paracentrotus lividus from Algerian west coast, applied to environmental monitoring. *Environ. Sci. Pollut. Res.* **2018**, *25*, 11238- 11251.
[30] Warnau M., Ledent G., Temaraa A., Bouquegneaub J-M., Jangouxatc M., Dubois P., Heavy metals in *Posidonia oceanica* and *Paracentrotus lividus* from seagrass beds of the north-western Mediterranean. *Sci. Total Environ.* **1995**, *171 (1-3),* 95-99.
[31] Warnau M, Teyssié JL, Fowler SW., Biokinetics of selected heavy metals and radionuclides in the common Mediterranean echinoid *Paracentrotus lividus:* sea water and food exposures. *Mar. Ecol. Prog. Ser.* **1996**, *141*, 83-94.
[32] Hayley M., Emberley J., Davis P.J., Morrow M.R., Robinson J.J., Interaction of Toposome from Sea-Urchin Yolk Granules with Dimyristoyl Phosphatidylserine Model Membranes: A ^{2}H-NMR Study. *Biophys J.* **2006,** *91 (12)*, 4555–4564.
[33] Castellano I., Migliaccio O., Ferraro G., Maffioli E., Marasco D., Merlino A., Zingone A., Tedeschi G., Palumbo A., Biotic and environmental stress induces nitration and changes in structure and function of the sea urchin major yolk protein toposome. *Sci. Rep.* **2018,** *8 (1)*, 4610.
[34] Noll H., Alcedo J., Daube M., Frei E., Schiltz E.,Hunt J.,Humphries T.,Matranga V., Hochstrasser M., Aebersold R., Lee H., Noll M., The toposome, essential for sea urchin cell adhesion and development, is a modified iron-less calcium-binding transferrin. *Dev. Biol.* **2007**, *310* (*1)*, 54-70.
[35] Cervello M., Matranga V., Evidence of a precursor-product relationship between vitellogenin and toposome, a glycoprotein complex mediating cell adhesion. *Cell. Differ. Dev.* **1989**, *26(1)*, 67-76.
[36] LLorens I., Solari P. L., Sitaud B., Bes R., Cammelli S., Hermange H., Othmane G., Safi S., Moisy P., Wahu S., Bresson C., Schlegel M. L., Menut D., Bechade J.-L., Martin P., Hazemann J.-L., Proux O., Den Auwer C., X-ray absorption spectroscopy investigations on radioactive matter using MARS beamline at SOLEIL synchrotron, *Radiochim. Acta* **2014**, *102 (11)*, 957–972.
[37] Ravel B., Newville M., ATHENA, ARTEMIS, HEPHAESTUS: data analysis for X-ray absorption spectroscopy using IFEFFIT, *J. Synchrotron Radiat.* **2005**, *12 (4)*, 537–541.
[38] Michalowicz A., Moscovici J., Muller-Bouvet D., Provost K., MAX: multiplatform applications for XAFS, *J. Phys.: Conf. Series*, **2009**, *190*, 012034.

[39] Bluhm H., Andersson K., Araki T., Benzerara K., Brown Jr. G. E., Dynes J. J., Ghosal S., Hansen H.-Ch., Hemminger J. C., Hitchcock A. P., Ketteler G., Kneedler E., Lawrence J. R., Leppard G. G., Majzlam J., Mun B. S., Myneni S. C. B., Nilsson A., Ogasawara H., Ogletree D. F., Pecher K., Shuh D. K., Salmeron M., Tonner B., Tyliszczak T., Yoon T. H., Soft X-ray Microscopy and Spectroscopy at the Molecular Environmental Science Beamline of the Advanced Light Source, *J. Electron Spectros. Rel. Phenom.* **2006**, *150 (2-3)*, 86-104.

[40] Maloubier M., Shuh D. K., Minasian S. G., Pacold J. I., Solari P.-L., Michel H., Oberhaensli F., Bottein Y., Monfort M., Moulin C., Den Auwer C., How do Radionuclides Accumulate in Marine Organisms? A Case Study of Europium with *Aplysina Cavernicola*, *Environ. Sci. Technol*. **2016**, *50 (19)*, 10730-10738.

[41] Dumas T., Guillaumont D., Fillaux C., Scheinost A., Moisy P., Petit S., Shuh D. K., Tyliszczak T., Den Auwer C., The Nature of Chemical Bonding in Actinide and Lanthanide Ferrocyanides Determined by X-ray Absorption Spectroscopy and Density Functional Theory, *Phys. Chem. Chem. Phys.* **2016**, *18 (4),* 2887-2895.

[42] http://unicorn.mcmaster.ca/aXis2000.html

[43] A. L. Drozdov V. V. Sharmankina L. A. Zemnukhova N. V. Polyakova. Chemical composition of spines and tests of sea urchins. *Biology Bull.* **2016**, *43 (6*), 521–531.

[44] Yohey S., Jillian F. Banfield Resistance to, and Accumulation of, Uranium by Bacteria from a Uranium-Contaminated Site. *Geomicrobiol. J.* **2004**, *21 (2)*, 113-121.

[45] Merroun M. L., Selenska-Pobell S., Bacterial interactions with uranium: An environmental perspective. *J. Contam. Hydrol.* **2008**, *102* (*3–4)*, 285-295.

[46] Pierrefite-Carle V, Santucci-Darmanin S, Breuil V, Gritsaenko T, Vidaud C, Creff G, Solari PL, Pagnotta S, Al-Sahlanee R, Den Auwer C, Carle GF., Effect of natural uranium on the UMR-106 osteoblastic cell line: impairment of the autophagic process as an underlying mechanism of uranium toxicity. *Arch Toxicol*. **2017**, *91 (4),* 1903-1914.

[47] Montavon G., Apostolidis C., Bruchertseifer F., Repinc U., Morgenstern A., Spectroscopic study of the interaction of U(VI) with transferrin and albumin for speciation of U(VI) under blood serum conditions. *J. Inorg. Biochem.* **2009**, *103 (12),* 1609–1616.

[48] Noll H., Matrangat V., Cervellot M., Humphreys T., Kuwasaki B., Adelson D., Characterization of toposomes from sea urchin blastula cells: A cell organelle mediating cell adhesion and expressing positional information. *Proc. Natl. Acad. Sci*. USA, **1985**, *82 (23),* 8062-8066.